I. SUPPLEMENTARY TABLES

Supplementary Table I. Table documenting processing time for various steps throughout the data acquisition and analysis pipeline.

Process	Software	Time/Sample (Minutes)	# Samples	Total Time (hours)
Morphometer Extraction	ImageJ	0.038	4250	2.69
Finite Element Analysis	MOOSE	73.08	654	796.57
Sample Concatenation	Python	0.006	654	0.07
Grid Search Optimization	Python, MATLAB	0.074	600	0.74
Final Model Training	MATLAB	0.002	600	0.02

Supplementary Table II. Table documenting data sources used for base CT scans.

Data Source	Description
Eckley[1]	4D Imaging of Acid Leaching in Porous Carbonado Diamond
Mascini[2]	4D micro-CT imaging of oil and waterflood in water and mixed-wet complex sandstones
Neumann[3]	11 Sandstones: raw, filtered and segmented data
Mohammadmoradi[4]	A Micro CT Image of Tight Carbonate
Ivonin[5]	A MicroCT Image of Silty Loam Phaeozem Albic
Mohammadmoradi[6]	A Multiscale Sandy Microstructure
Rucker[7]	A Time-Resolved Synchrotron X-Ray Micro-Tomography Dataset of a Waterflood in an Altered Mixed-Wet Ketton Limestone
Heidari[8]	Austin Chalk
Bultreys[9]	Belgian Fieldstone
Ferreira[10]	Carbonates: Porosity and Permeability Voxel to Voxel
Lin[11]	Data for Pore-Scale Imaging of Displacement Patterns in an Altered-Wettability Carbonate
Wang[12]	Dataset for Unsteady-State Capillary Drainage experiment on Estaillades Carbonate
Andrew[13]	Doddington Sandstone
Ni[14]	Drainage Experiment in an Intermediate-Scale Beadpack
Bultreys[15]	Estaillades Carbonate #2
Crandall[16]	Foamed Cement API RP 10B-4
Ketcham[17]	Fracture in Granite
Luo[18]	Fracture Patterns in Laminated Mancos Shale
Berg[19]	Gildehauser Sandstone
Chen[20]	Grain-scale Failure Mechanism of a Porous Sandstone in Brazilian Tensile Test
Chen[21]	Hydrate-Bearing Sand
Karpyn[22]	Induced Rough Fracture in Berea Sandstone Core
Moon[23]	Intergranular Pore Structures in Sandstones
Dalton[24]	Laboratory Foamed-Cement-Curing Evolution Using CT Scanning: Insights from Elevated-Pressure Generation
Bultreys[25]	Massangis Jaune Carbonate
Patmonoaji[26]	Micro-tomographic Imaging of the Dissolution of Trapped Nitrogen Gas with and without Dissolution Fingering
Beckingham[27]	Paluxy Sandstone
Pradanovic[28]	Partially Cemented Tight Sandstone Fracture
Khan[29]	Particulate Straining in Simple Porous Media
Karpyn[30]	Pore Scale Multiphase Flow Experiments in Bead Packs of Variable Wettability
Dalton[31]	Sessile Drop and Micro-CT Data for Six Sandstone Formations
Mehmani[32]	Wilcox Tight Gas Sandstone
Saur[33]	X-ray Micro-CT Images of Calcareous Shale Samples

Supplementary Table III. Table indicating which extracted geometric features were compared against Minkowski functionals.

Feature Name	Description
Volume Density	Shape volume normalized by total volume of the sampling window
Surface Area Density	Shape surface area normalized by total volume of the sampling window
Mean Breadth Density	Average of caliper diameter over all directions normalized by total volume of the sampling window
Euler Number Density	Euler number of the shape normalized by total volume of the sampling window
Grain Count	Number of grains in 3D reconstruction
Volume	Number of voxels in 3D reconstruction multiplied by volume of one voxel
Surface Area	Surface area of shape
Mean Breadth	Average caliper diamter over all directions
Sphericity	Ratio of squared volume over the cube of the surface area
Euler Number	Descriptor of region topology (connected components minus number of holes)
Box X. Min.	Smallest Feret diameter in the X direction
Box X. Max.	Largest Feret diameter in the X direction
Box Y. Min.	Smallest Feret diameter in the Y direction
Box Y. Max.	Largest Feret diameter in the Y direction
Box Z. Min.	Smallest Feret diameter in the Z direction
Box Z. Max.	Largest Feret diameter in the Z direction
Centroid X	X-coordinate of the shape centroid
Centroid Y	Y-coordinate of the shape centroid
Centroid Z	Z-coordinate of the shape centroid
Ellipse Center X	X-coordinate of the inertial ellipse centroid
Ellipse Center Y	Y-coordinate of the inertial ellipse centroid
Ellipse Center Z	Z-coordinate of the inertial ellipse centroid
Ellipsoid Radius 1	Length of the largest semi-axis of the inertial ellipse
Ellipsoid Radius 2	Length of the medium semi-axis of the inertial ellipse
Ellipsoid Radius 3	Length of the smallest semi-axis of the inertial ellipse
Ellipsoid Azimuth	Azimuth of the projection of the major axis on the XY plane of the inertial ellipse, in degrees
Ellipsoid Elevation	Elevation of the major axis on the XY plane of the inertial ellipse, in degrees
Ellipsoid Roll	Rotation of the inertial ellipsoid around the main axis, in degrees
Ellipsoid R1/R2	Ratio of Radius 1 to Radius 2 of the inertial ellipse
Ellipsoid R1/R3	Ratio of Radius 1 to Radius 3 of the inertial ellipse
Ellipsoid R2/R3	Ratio of Radius 2 to Radius 3 of the inertial ellipse
Inscribed Ball X	The X-coordinate of the mean largest sphere that can fit in a corresponding grain
Inscribed Ball Y	The Y-coordinate of the mean largest sphere that can fit in a corresponding grain
Inscribed Ball Z	The Z-coordinate of the mean largest sphere that can fit in a corresponding grain
Inscribed Ball Radius	The mean radius of the largest sphere that can fit in a corresponding grain

II. SUPPLEMENTARY FIGURES

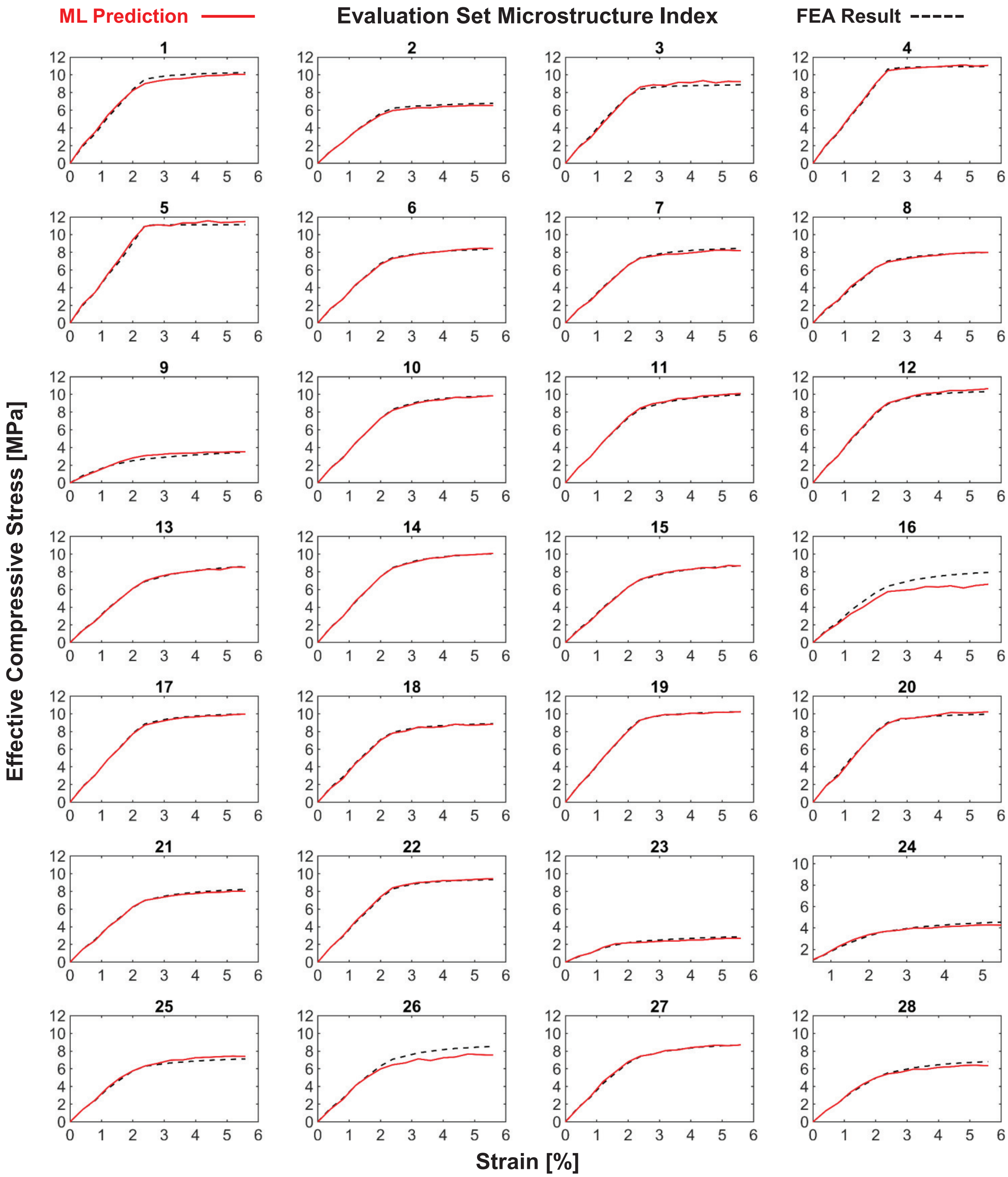

Supplementary Figure 1. Predicted and simulated compressive stress-strain curves for evaluation set samples 1-28.

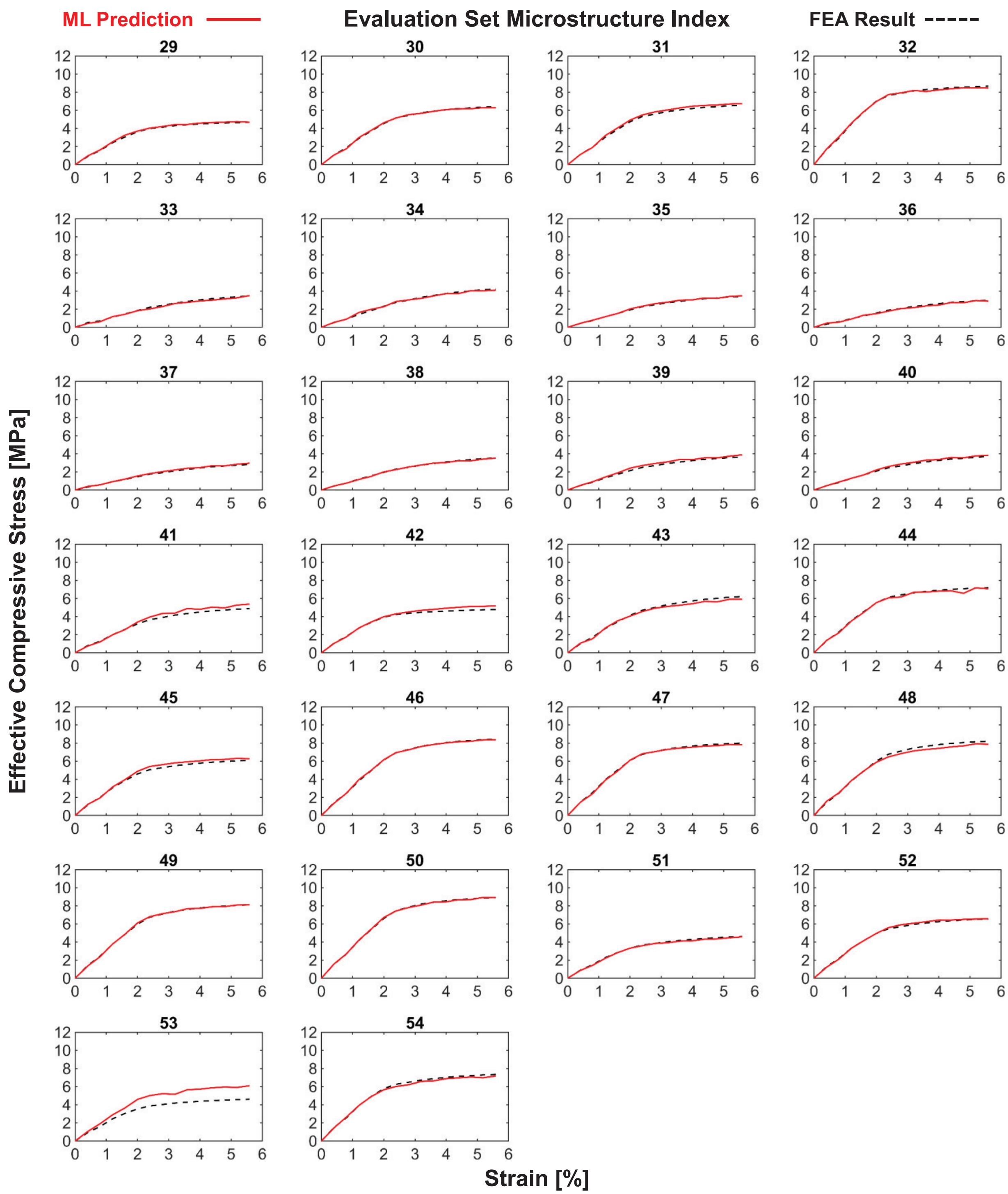

Supplementary Figure 2. Predicted and simulated compressive stress-strain curves for evaluation set samples 29-54.

REFERENCES

[1] S. Eckley and R. Ketcham, "4d imaging of acid leaching in porous carbonado diamond," http://www.digitalrocksportal.org/projects/219 (2019).

[2] A. Mascini, M. Boone, S. Wang, S. Van Offenwert, V. Cnudde, and T. Bultreys, "4d micro-ct imaging of oil- and waterflood in water- and mixed-wet complex sandstones," http://www.digitalrocksportal.org/projects/378 (2021).

[3] R. Neumann, M. Andreeta, and E. Lucas-Oliveira, "11 sandstones: raw, filtered and segmented data," http://www.digitalrocksportal.org/projects/317 (2020).

[4] P. Mohammadmoradi, "A micro ct image of tight carbonate," http://www.digitalrocksportal.org/projects/118 (2017).

[5] D. Ivonin and T. Kalnin, "A microct image of silty loam phaeozem albic," http://www.digitalrocksportal.org/projects/302 (2020).

[6] P. Mohammadmoradi, "A multiscale sandy microstructure," http://www.digitalrocksportal.org/projects/92 (2017).

[7] M. Rücker, W.-B. Bartels, S. Berg, F. Enzmann, A. Jacob, H. Mahani, N. Brussee, C. Hinz, A. Georgiadis, and C. Wagner, "A time-resolved synchrotron x-ray micro-tomography dataset of a waterflood in an altered mixed-wet ketton limestone," http://www.digitalrocksportal.org/projects/202 (2019).

[8] Z. Heidari and A. Posenato Garcia, "Austin chalk," http://www.digitalrocksportal.org/projects/35 (2016).

[9] T. Bultreys and W. De Boever, "Belgian fieldstone," http://www.digitalrocksportal.org/projects/297 (2020).

[10] L. Ferreira, R. Surmas, M. Silva, and R. Peçanha, "Carbonates: Porosity and permeability voxel to voxel," http://www.digitalrocksportal.org/projects/252 (2020).

[11] Q. Lin, B. Bijeljic, S. Berg, and M. Blunt, "Data for pore-scale imaging of displacement patterns in an altered-wettability carbonate," http://www.digitalrocksportal.org/projects/331 (2020).

[12] S. Wang, T. Bultreys, S. Van Offenwert, and L. Ruspini, "Dataset for unsteady-state capillary drainage experiment on estaillades carbonate," http://www.digitalrocksportal.org/projects/363 (2021).

[13] M. Andrew, B. Bijeljic, and M. Blunt, "Doddington sandstone," http://www.

digitalrocksportal.org/projects/290 (2020).

[14]H. Ni and T. Meckel, "Drainage experiment in an intermediate-scale beadpack," http://www.digitalrocksportal.org/projects/379 (2021).

[15]T. Bultreys, "Estaillades carbonate #2," http://www.digitalrocksportal.org/projects/58 (2016).

[16]D. Crandall, S. Fuchs, M. Gill, J. Moore, and B. Kutchko, "Foamed cement api rp 10b-4," http://www.digitalrocksportal.org/projects/154 (2018).

[17]R. Ketcham, M. Colbert, J.-Q. Zhou, and B. Cardenas, "Fracture in granite," http://www.digitalrocksportal.org/projects/195 (2018).

[18]J. Luo, M. Ramos, and D. N. Espinoza, "Fracture patterns in laminated mancos shale," http://www.digitalrocksportal.org/projects/205 (2019).

[19]S. Berg, R. Armstrong, and A. Wiegmann, "Gildehauser sandstone," http://www.digitalrocksportal.org/projects/134 (2018).

[20]B. Chen, "Grain-scale failure mechanism of a porous sandstone in brazilian tensile test," http://www.digitalrocksportal.org/projects/250 (2019).

[21]X. Chen, D. N. Espinoza, M. Prodanovic, and R. Verma, "Hydrate-bearing sand," http://www.digitalrocksportal.org/projects/122 (2017).

[22]Z. Karpyn, C. Landry, and M. Prodanovic, "Induced rough fracture in berea sandstone core," http://www.digitalrocksportal.org/projects/31 (2016).

[23]C. Moon and M. Andrew, "Intergranular pore structures in sandstones," http://www.digitalrocksportal.org/projects/222 (2019).

[24]L. E. Dalton, S. Brown, J. Moore, D. Crandall, and M. Gill, "Laboratory foamed-cement-curing evolution using ct scanning: insights from elevated-pressure generation," SPE Drilling & Completion **34**, 81–91 (2019).

[25]T. Bultreys, "Massangis jaune carbonate," http://www.digitalrocksportal.org/projects/73 (2016).

[26]A. Patmonoaji, Y. Hu, M. Nasir, C. Zhang, and T. Suekane, "Micro-tomographic imaging of the dissolution of trapped nitrogen gas with and without dissolution fingering," http://www.digitalrocksportal.org/projects/359 (2021).

[27]L. Beckingham, I. Anjikar, and F. Qin, "Paluxy sandstone," http://www.digitalrocksportal.org/projects/196 (2019).

[28]M. Prodanovic, A. Tokan-Lawal, and P. Eichhubl, "Partially cemented tight sandstone fracture,"

http://www.digitalrocksportal.org/projects/5 (2015).

[29] H. Khan, M. Prodanovic, and D. Dicarlo, "Particulate straining in simple porous media," http://www.digitalrocksportal.org/projects/51 (2016).

[30] Z. Karpyn, "Pore scale multiphase flow experiments in bead packs of variable wettability," http://www.digitalrocksportal.org/projects/189 (2018).

[31] L. Dalton, "Sessile drop and micro-ct data for six sandstone formations," url-http://www.digitalrocksportal.org/projects/255 (2020).

[32] A. Mehmani, M. Prodanovic, and K. L. Milliken, "Wilcox tight gas sandstone," http://www.digitalrocksportal.org/projects/6 (2015).

[33] H. Saur, C. Aubourg, and P. Moonen, "X-ray micro-ct images of calcareous shale samples," http://www.digitalrocksportal.org/projects/370 (2021).